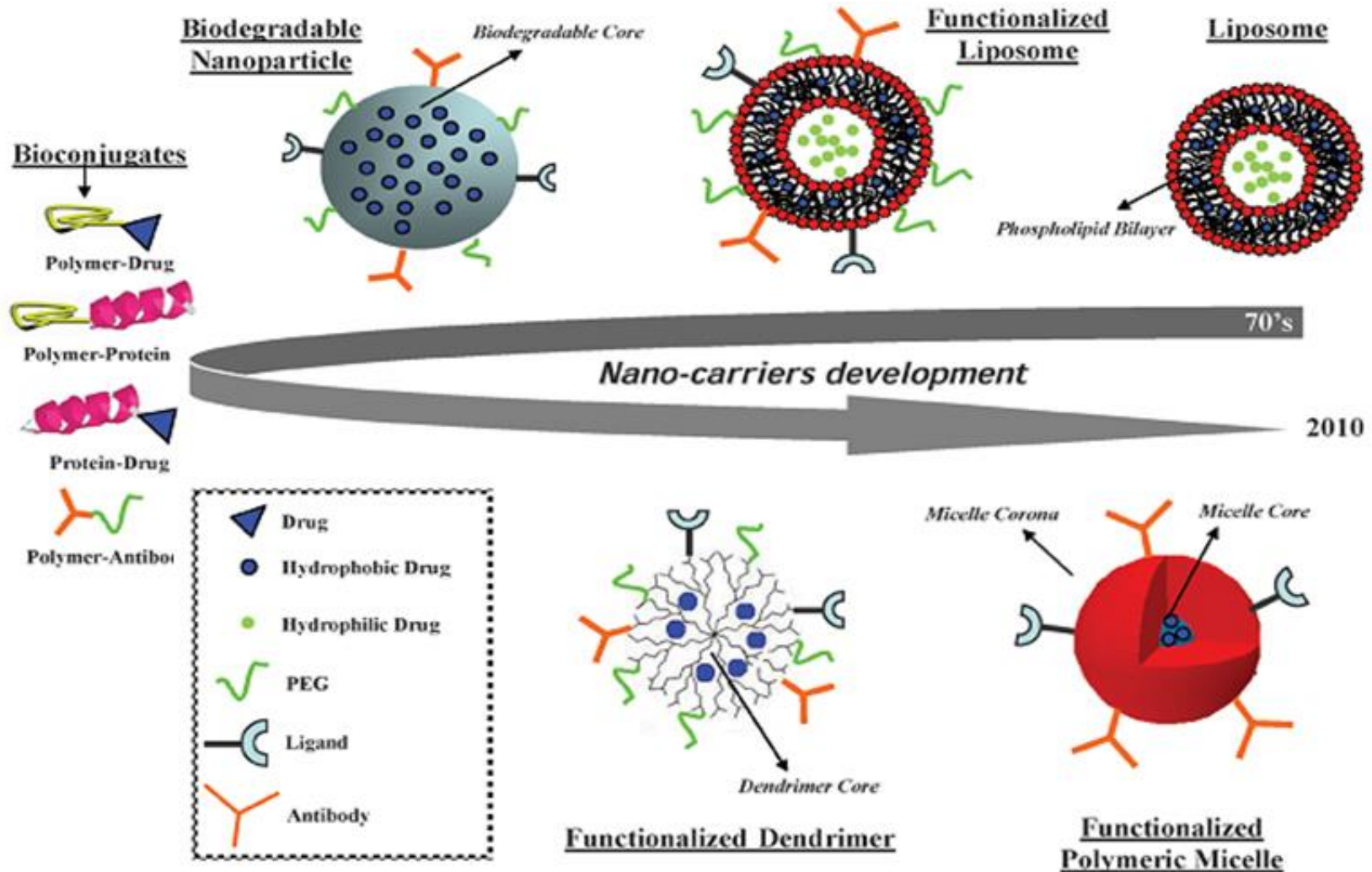# Improvement of Nanoparticle Drug Delivery by Surface Conjugation with L-carnitine: Role of OCTN2/SLC22A5 and ATB$^{0,+}$/SLC6A14

Vadivel Ganapathy, Ph. D.
Department of Cell Biology and Biochemistry
Texas Tech University Health Sciences Center
Lubbock, TX, USA

Development of nano-drug delivery systems

Tumor-selective delivery of nanoparticles

Nanoparticle delivery
- → **Passive**
- → **Active**

Active Delivery

Cell-surface receptors

Receptor	Ligand
TfR	Transferrin
LDLR	LDL
EGFR	EGF
EGFR	EGFRmAb
Folate receptor	Folic acid
LRP-1	Angiopep-2
Neonatal FcR	IgG Fc fragment

Cell-surface transporters

Transporter	Ligand
GLUT1	D-Glucose 2-Deoxy-D-glucose Dehydroascorbic acid
CTL	Choline
LAT1	γ-Carboxy-linked glutamate
OCTN2	Carnitine
$ATB^{0,+}$	Carnitine Lysine

Transporter-assisted delivery of nanoparticles across the BBB
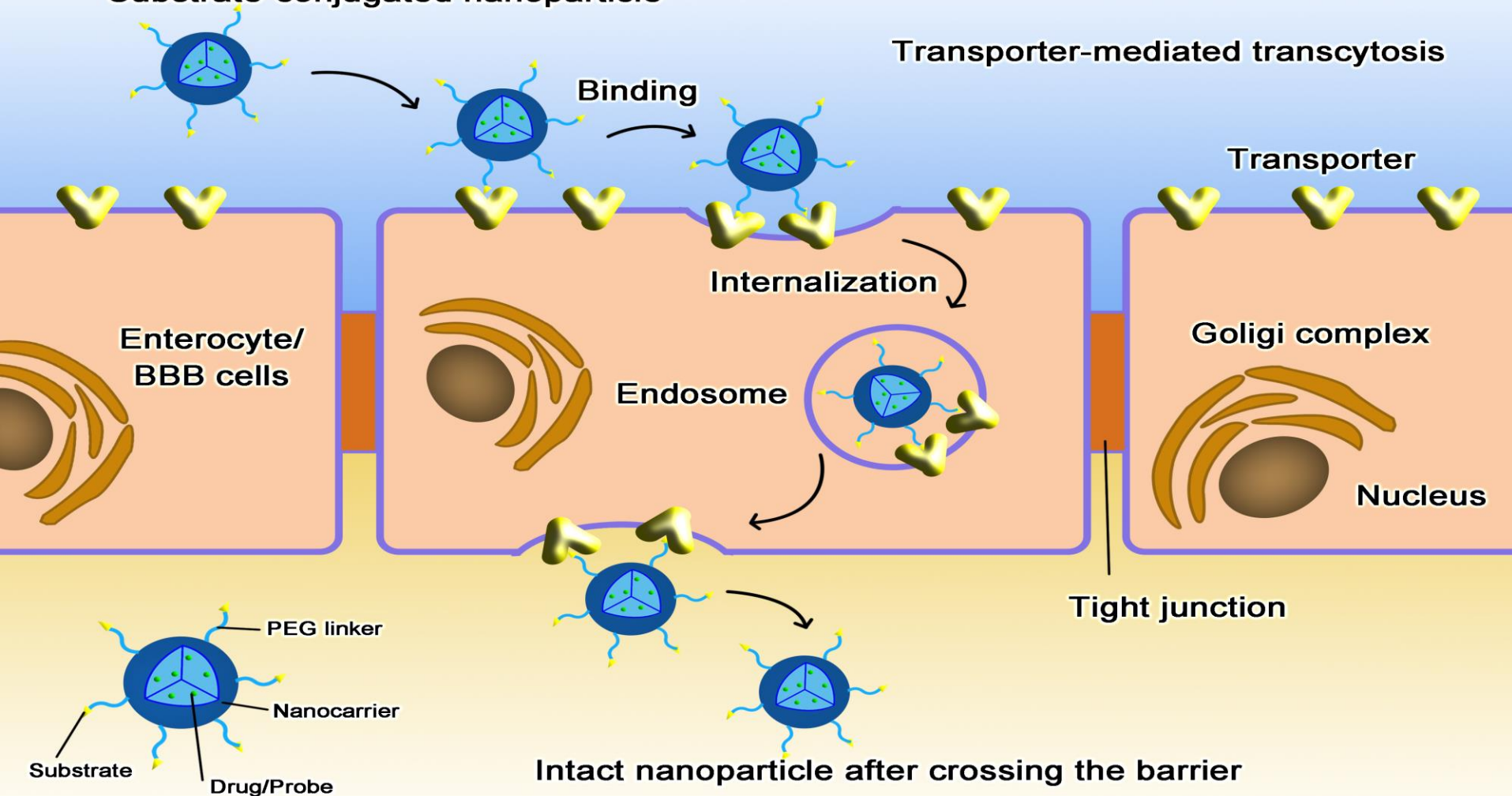
Transporter-targeted nanoparticles for enhanced BBB permeation and glioma targeting

Table 1. Transporter-targeted nanoparticles to enhance blood-brain barrier permeation and increase glioma targeting for optimal anti-glioma therapy.

Transporter	Gene	Substrate	Carrier	Drug	Ref.
GLUT1	SLC2A1	2-deoxy-D-glucose	nanoparticles	Paclitaxel	(Jiang et al., 2014b)
		D-glucosamine	nanoparticles	Paclitaxel	(Jiang et al., 2014a)
		dehydroascorbic acid	Micelles	Paclitaxel	(Shao et al., 2014)
ChT1	SLC5A7	Choline derivate	Dendrimers	Plasmid DNA	(Li et al., 2011)
			Dendrimers	DTPA-Gd	(Li et al., 2013b)
			Micelles	Doxorubicin/Plasmid DNA	(Li et al., 2013a)
LAT1	SLC7A5	Glutamate	Micelles	Doxorubicin	(Li et al., 2015)
			Liposomes	Docetaxel	(Li et al., 2016)
SVCT2	SLC23A2	Vitamin C	Micelles	Rhodamine	(Salmaso et al., 2009)

Transporter-targeted nanoparticles for site-specific absorption

Table 2. Transporter-targeted nanoparticles for increased site-specific absorption

Transporter	Gene	Substrate	Carrier	Drug	Site	Ref.
GLUT1	SLC2A1	2-deoxy-D-glucose	DMSA-DG NPs	γ-Fe_2O_3	Tumor	(Shan et al., 2012)
		Glucose	Nanoparticles	Coumarin 6	Brain	(Xie et al., 2012)
GLUT4	SLC2A4	Glucose	Quantum dots		Muscle	(Yeh et al., 2014)
SMVT	SLC5A6	Biotin	Dendrimer	FITC	Tumor	(Yang et al., 2009; Yellepeddi et al., 2009)
			Dendrimer	Cisplatin	Ovarian cancer	(Yellepeddi et al., 2011)
			Pullulan acetate nanoparticles	Doxorubicin	Tumor	(Na et al., 2003)
			Polymer micelles	Doxorubicin	Tumor	(Kim et al., 2012)
			Erythrocytes	Methotrexate	Liver	(Mishra and Jain, 2002)
			Cubosomes	Paclitaxel, MO-Fluo	Tumor	(Aleandri et al., 2015)
			Polyurethane-urea nanoparticles	Sunitinib/phenoxodiol, plasmid DNA	hepatocellular carcinoma	(Morral-Ruíz et al., 2015)
ATB$^{0,+}$	SLC6A14	Lysine	Liposomes	Docetaxel	Liver cancer	(Luo et al., 2016)
		Aspartate	Liposomes	Docetaxel	Lung cancer	(Luo et al., 2017)
LAT1	SLC7A5	Glutamate	Nanoparticles	Paclitaxel	Breast cancer	(Li et al., 2017)
MCT1	SLC16A1	β-hydroxybutyrate	Solid lipid nanoparticles	Docetaxel	Brain	(Venishetty et al., 2013)

Transporter-targeted nanoparticles for enhanced oral absorption

Table 3. Transporter-targeted nanoparticles for enhanced oral absorption

| Transporter	Gene	Substrate	Carrier	Drug	Ref.
SMVT	SLC5A6	Biotin	Conjugates	Peptide	(Ramanathan et al., 2001a; Ramanathan et al., 2001b)
			Conjugates	Camptothecin	(Minko et al., 2002)
			Liposomes	Insulin	(Zhang et al., 2014)
			Solid lipid nanoparticles	Oridonin	(Zhou et al., 2015)
ASBT	SLC10A2	Deoxycholic acid	Conjugates	LMWH	(Lee et al., 2001; Lee et al., 2006; Kim et al., 2007)
		Deoxycholic acid	Conjugates	Insulin	(Lee et al., 2005a)
		TetraDOCA	Conjugates	LHT7	(Alam et al., 2014)
		Taurocholic acid	Micelles	Docetaxel	(Khatun et al., 2013)

OCTN2/SLC22A5
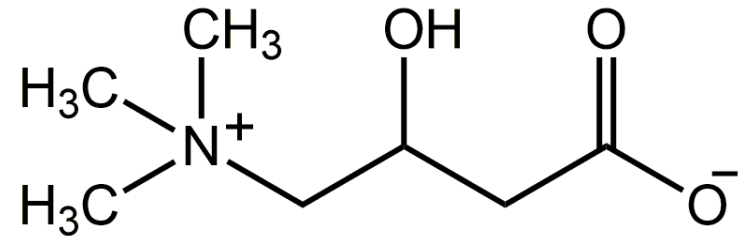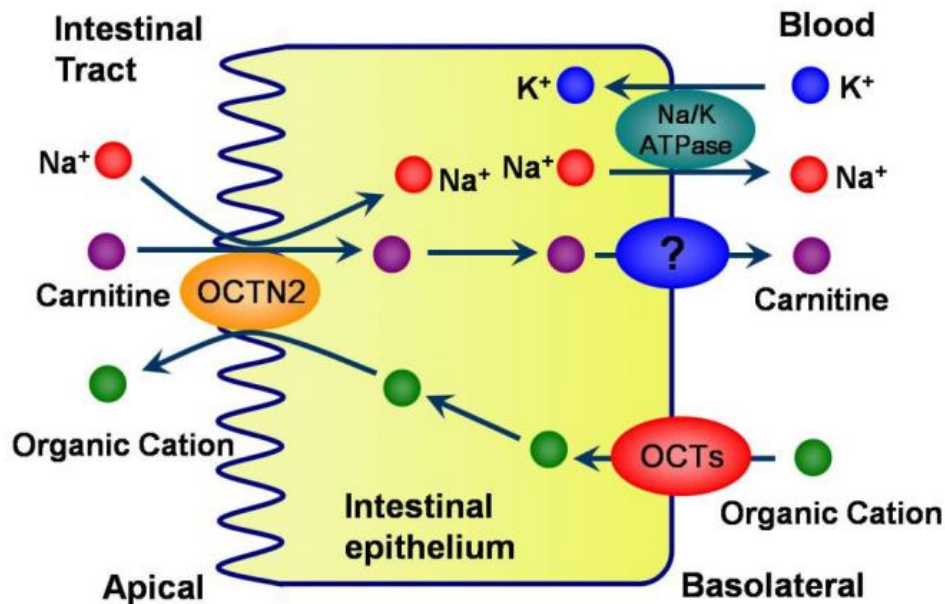
L-Carnitine

- Advantages of OCTN2 as a target for oral delivery

- Wide absorption window (small intestine and colon)

- Na-coupled and active

- L-Carnitine is easy to link

L-Carnitine-conjugated NPs
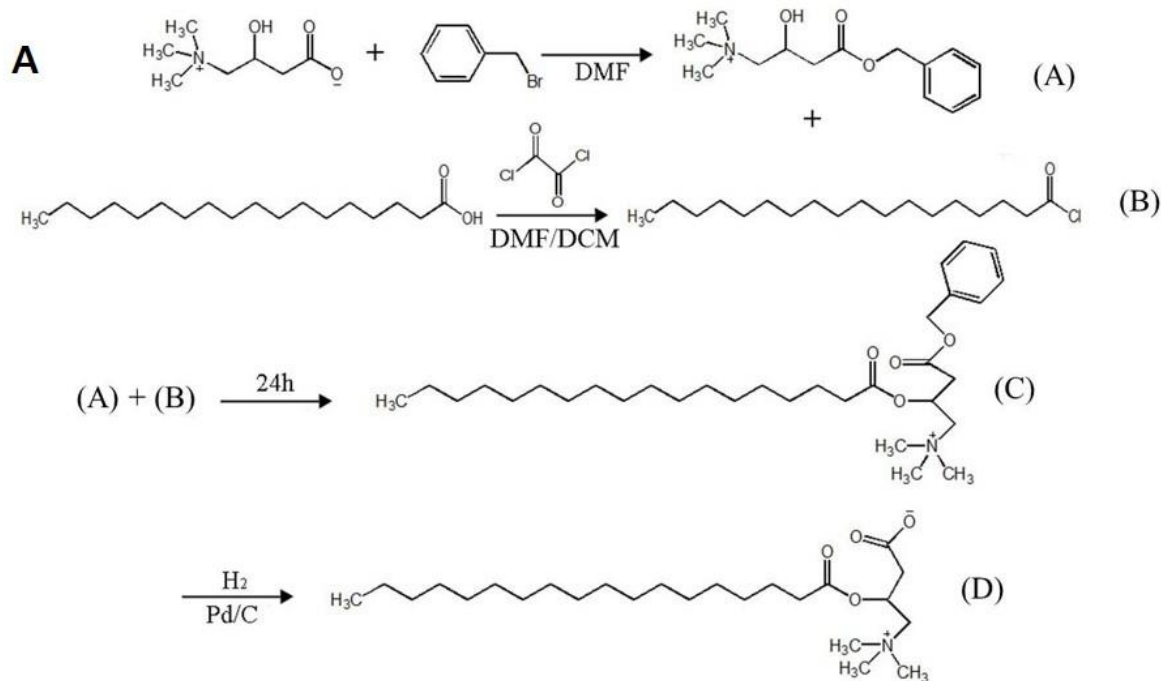
- Synthetic route of stearoyl-L-carnitine
- Characterization of stearoyl-L-carnitine by ^{1}H NMR spectrum in CDCl$_3$;
- Characterization of stearoyl-L-carnitine by MS.
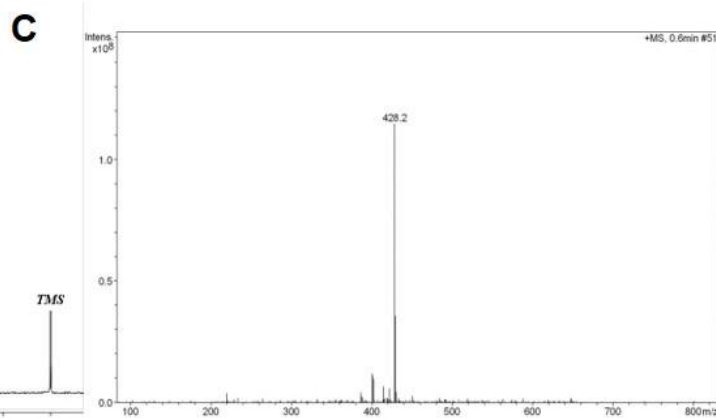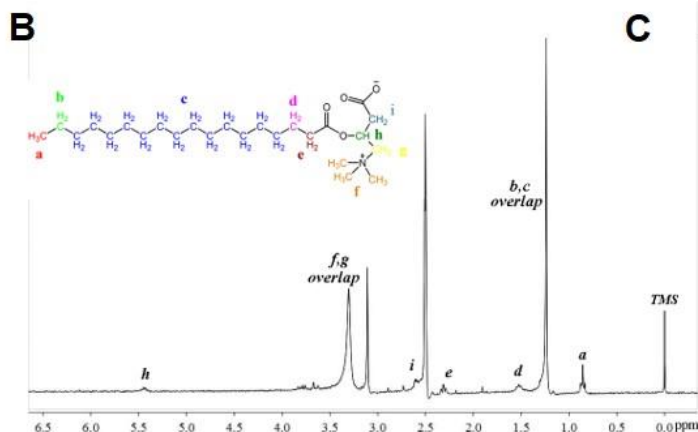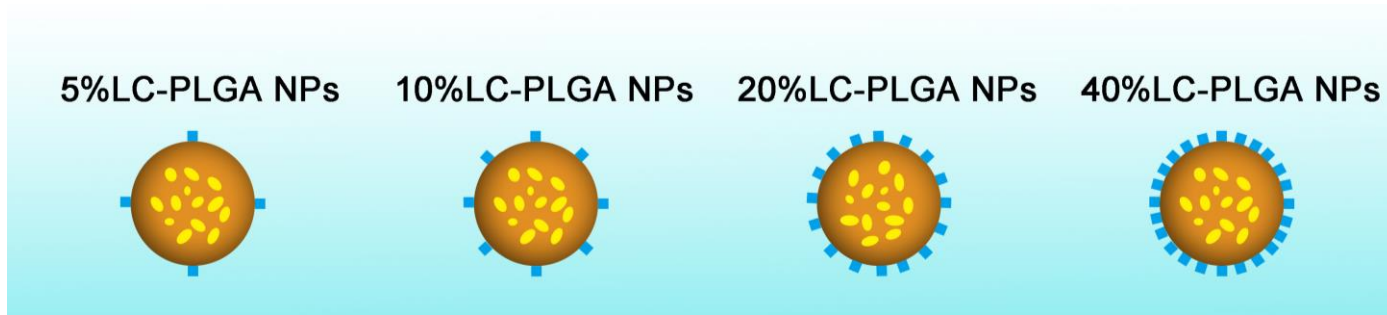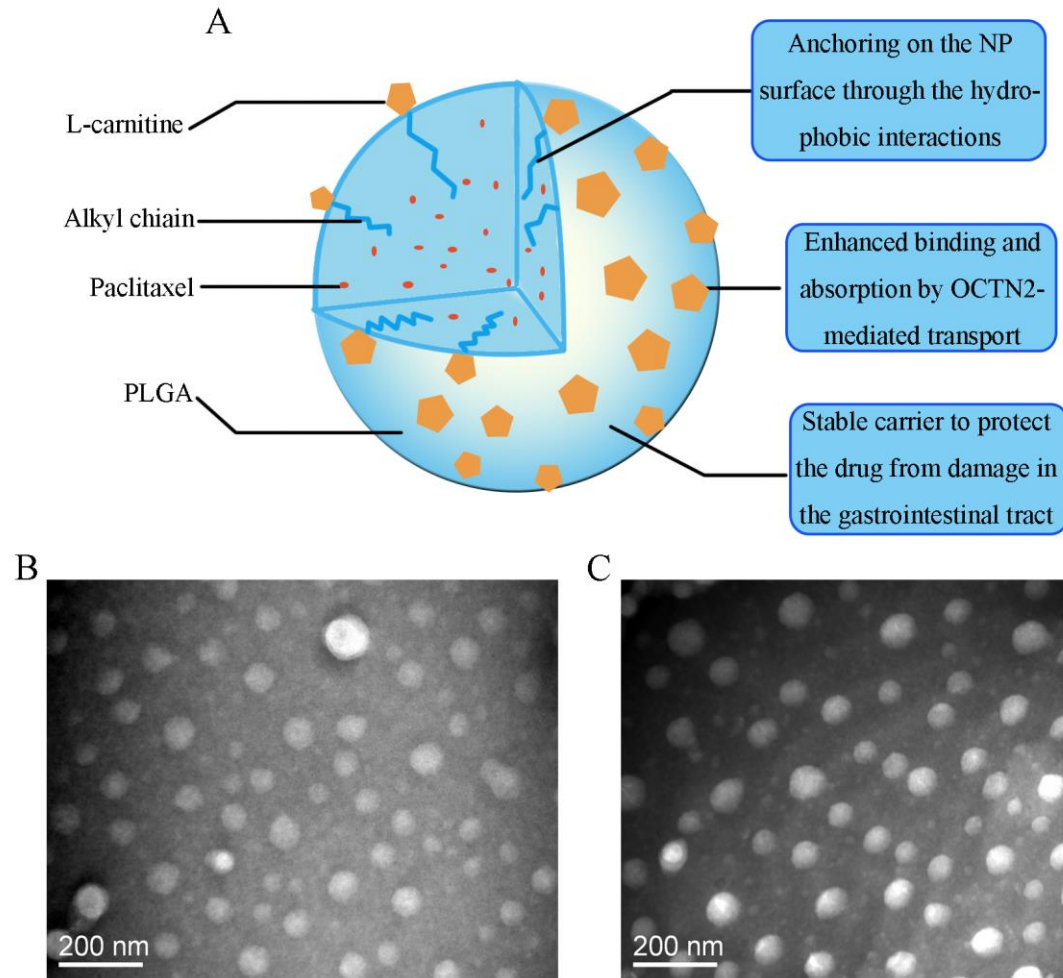
L-Carnitine-conjugated NPs: Characteristics

**Table 1-1**. Physicochemical characterization of LC-PLGA NPs.

nanoparticles	Size (nm)	PDI	Zeta potential (mV)	EE%	DL%
PLGA NPs	211.3±1.4	0.079±0.029	-4.42±0.70	91.4±3.2	4.35±0.15
5%LC-PLGA NPs	201.1±4.4	0.101±0.047	-0.99±0.08	98.8±2.8	4.70±0.13
10%LC-PLGA NPs	197.5±5.4	0.175±0.021	-0.36±0.08	98.0±1.6	4.67±0.08
20%LC-PLGA NPs	205.0±2.7	0.076±0.048	-0.57±0.15	77.8±0.1	3.71±0.00
40%LC-PLGA NPs	202.2±2.5	0.161±0.024	1.33±0.34	71.8±2.0	3.42±0.09

L-Carnitine-conjugated NPs: Characteristics

Schematic illustration of paclitaxel-loaded LC-PLGA NPs (A), and TEM images of PLGA-NPs (B) and LC-PLGA-NPs (C).

L-Carnitine-conjugated NPs: Uptake in Caco-2 cells
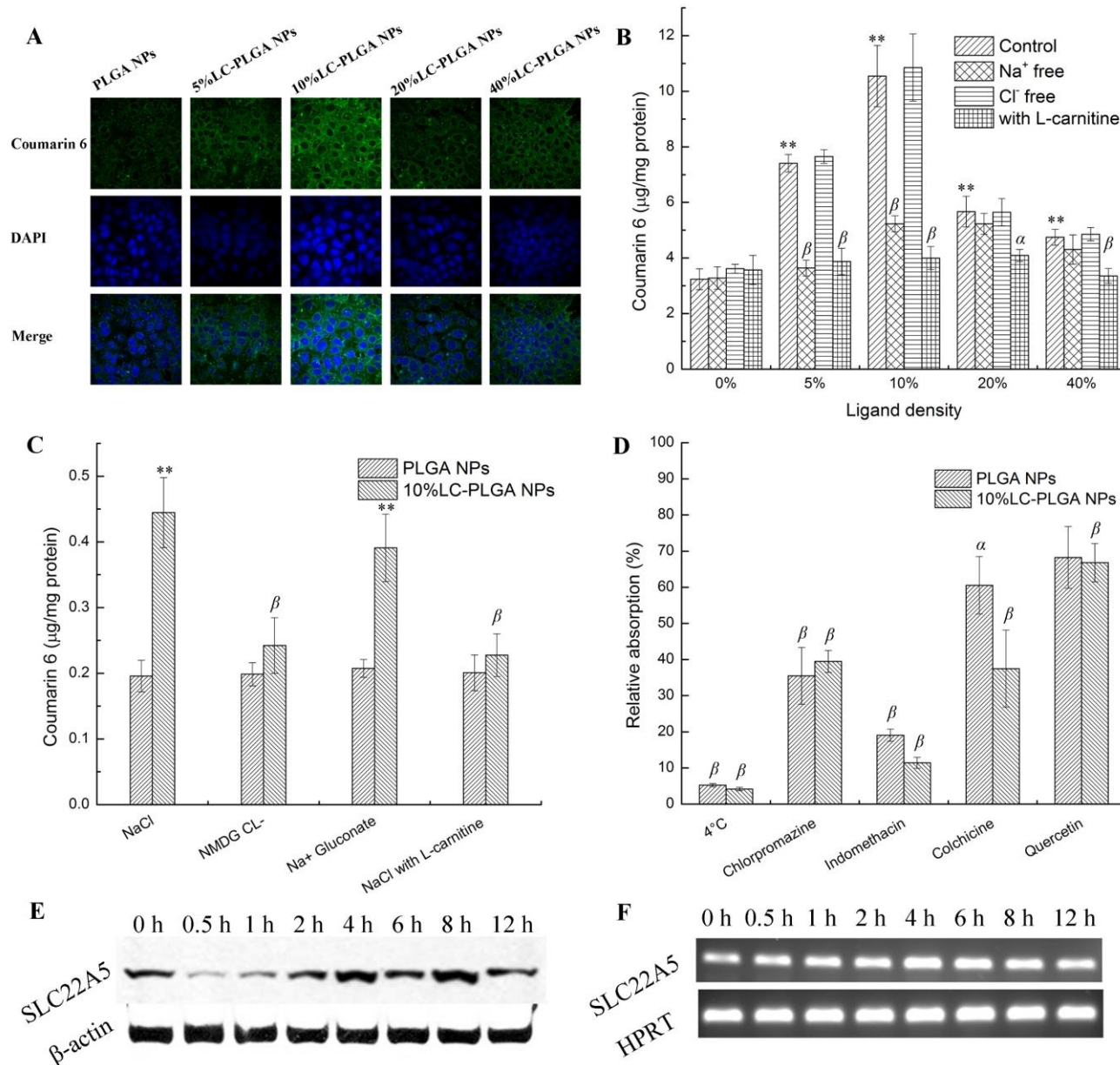
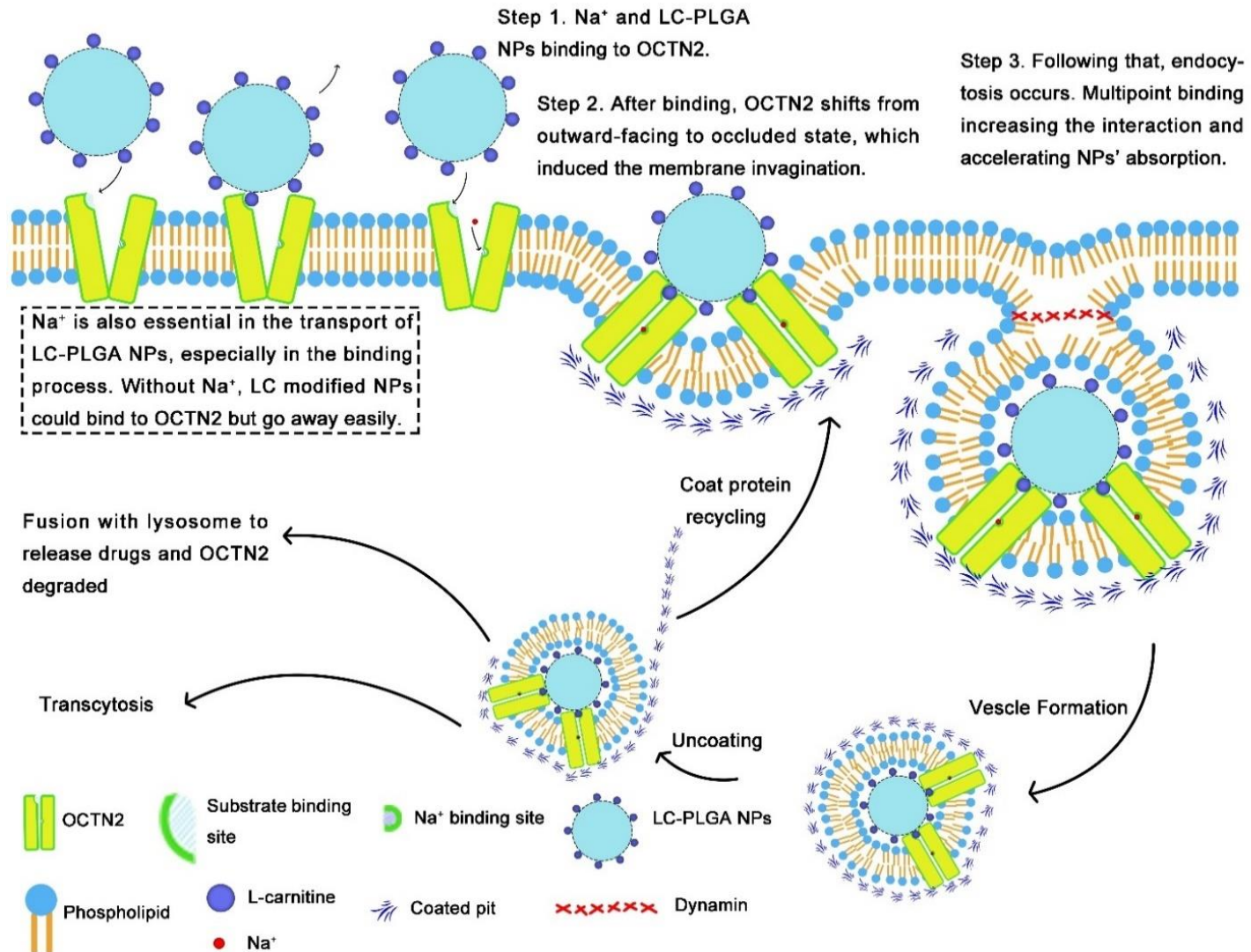
Characteristics of nanoparticles uptake in Caco-2 cells.

(A) Confocal microscope images of Caco-2 cells incubated with LC-PLGA NPs at 37 ° C for 1 h

(B) Uptake assay for LC-PLGA NPs in different buffers in Caco-2 cells

(C) Binding assay

(D) Endocytosis study

(E) Western bolt

(F) RT-PCR study

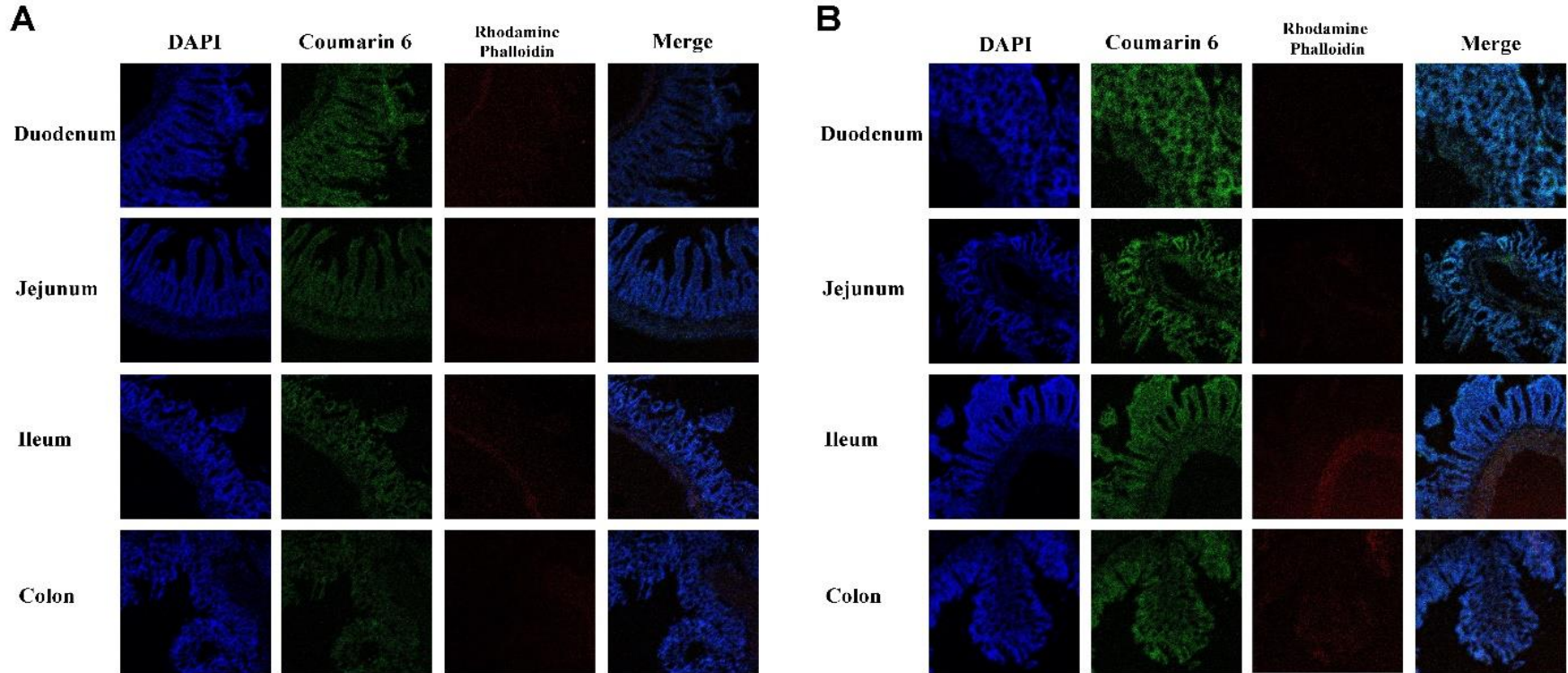# L-Carnitine-conjugated NPs: Influence of ligand density
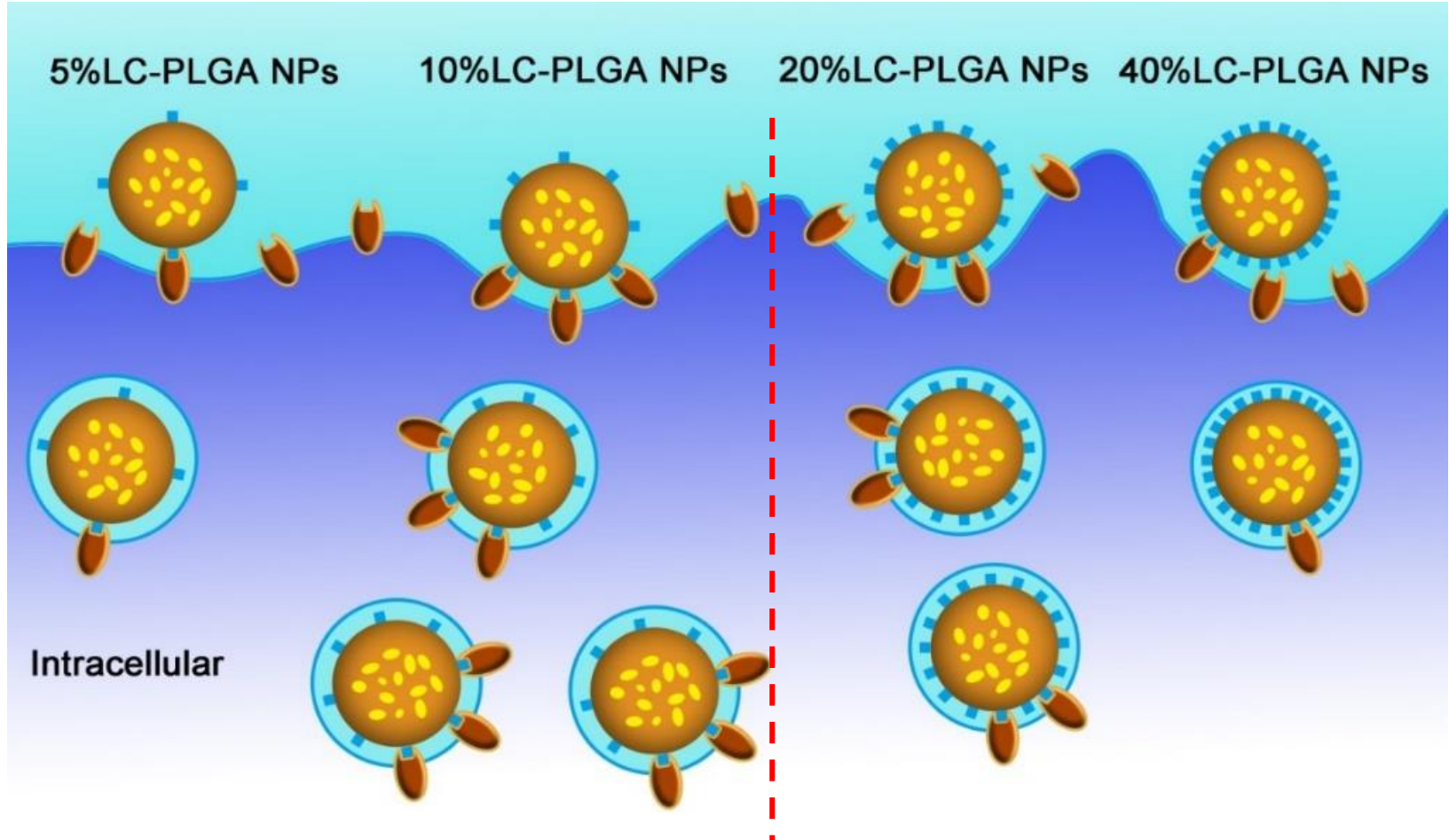
Effects of the ligand density on the nanoparticle absorption: when ligand density was low, the increased ligand density could enhance absorption; when ligand density was enough, the further increased ligand might inhibit the binding of nanoparticles to target site (too crowd).

# L-Carnitine-conjugated NPs: OCTN2-mediated entry into cells

Step 1. Na⁺ and LC-PLGA NPs binding to OCTN2.

Step 2. After binding, OCTN2 shifts from outward-facing to occluded state, which induced the membrane invagination.

Step 3. Following that, endocytosis occurs. Multipoint binding increasing the interaction and accelerating NPs' absorption.

Na⁺ is also essential in the transport of LC-PLGA NPs, especially in the binding process. Without Na⁺, LC modified NPs could bind to OCTN2 but go away easily.

Coat protein recycling

Fusion with lysosome to release drugs and OCTN2 degraded

Transcytosis

Uncoating

Vescle Formation

OCTN2   Substrate binding site   Na⁺ binding site   LC-PLGA NPs

Phospholipid   L-carnitine   Coated pit   ✗✗✗✗✗ Dynamin   Na⁺

L-Carnitine-conjugated NPs: Intestinal absorption

The fluorescence images of rat intestinal sections after oral administration of coumarin 6-loaded A) PLGA NPs and B) 10%LC-PLGA NPs. Blue: DAPI for nuclei, Green: coumarin 6, Red: rhodamine phalloidin for cytoskeleton.
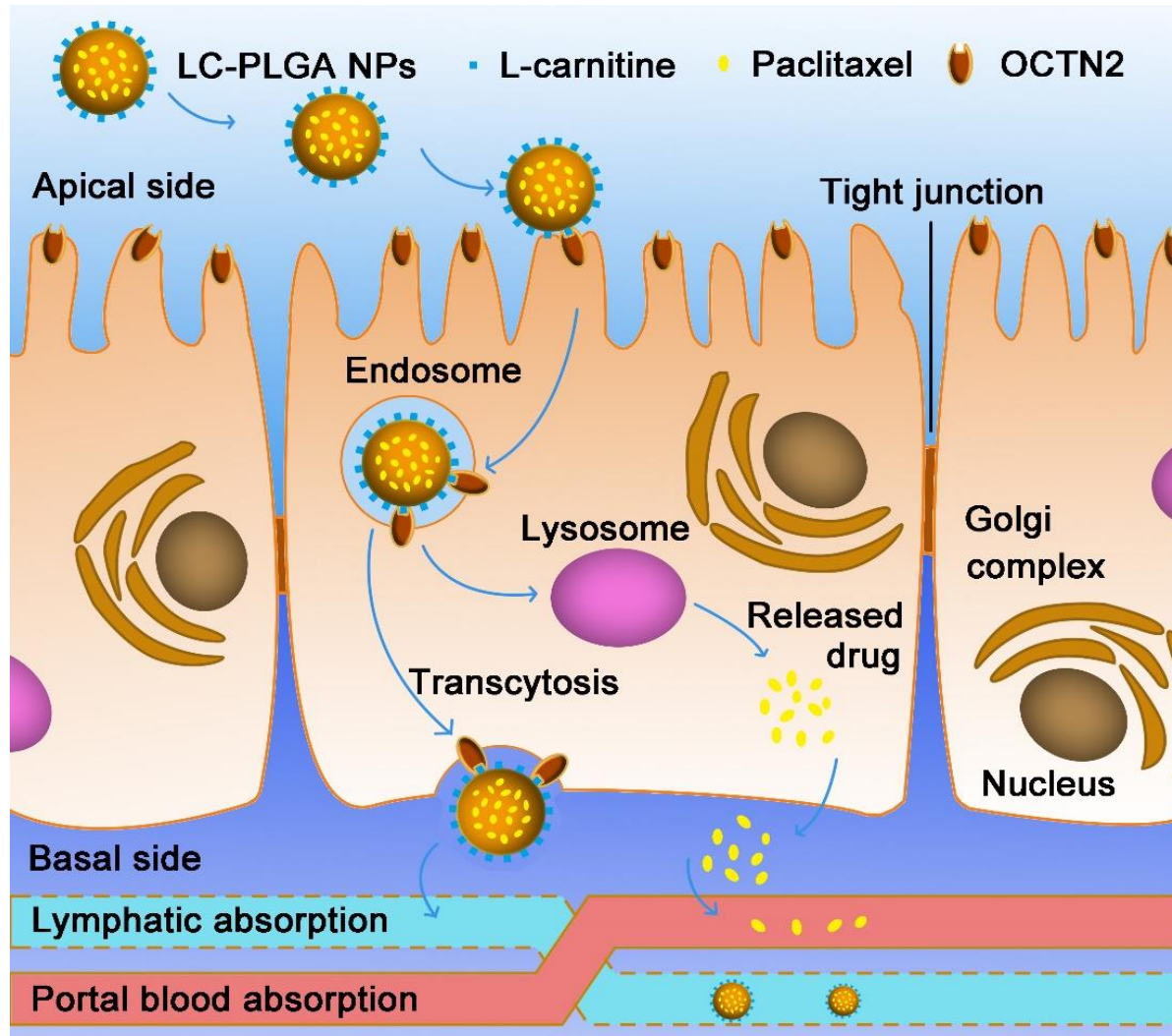
L-Carnitine-conjugated NPs: Intestinal permeability
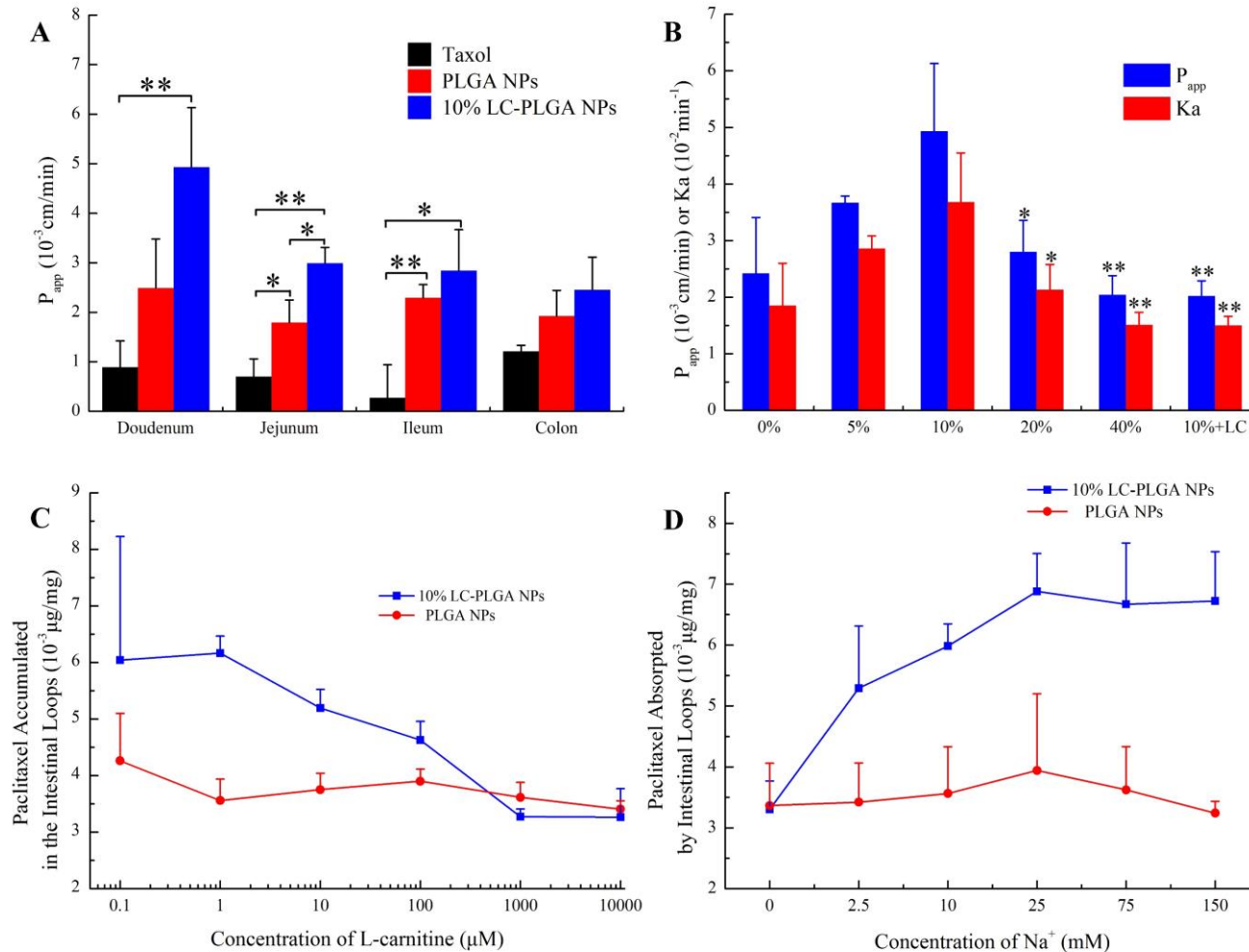
(A) The intestinal permeabilities (Papp) different formulations; (B) The effect of surface density of L-carnitine conjugation on in situ intestinal absorption; (C) Influence of free L-carnitine on the absorption of LC-PLGA NPs in everted intestinal rings; (D) Influence of Na^+ on the absorption of LC-PLGA NPs in everted intestinal rings.

L-Carnitine-conjugated NPs: Intestinal absorption
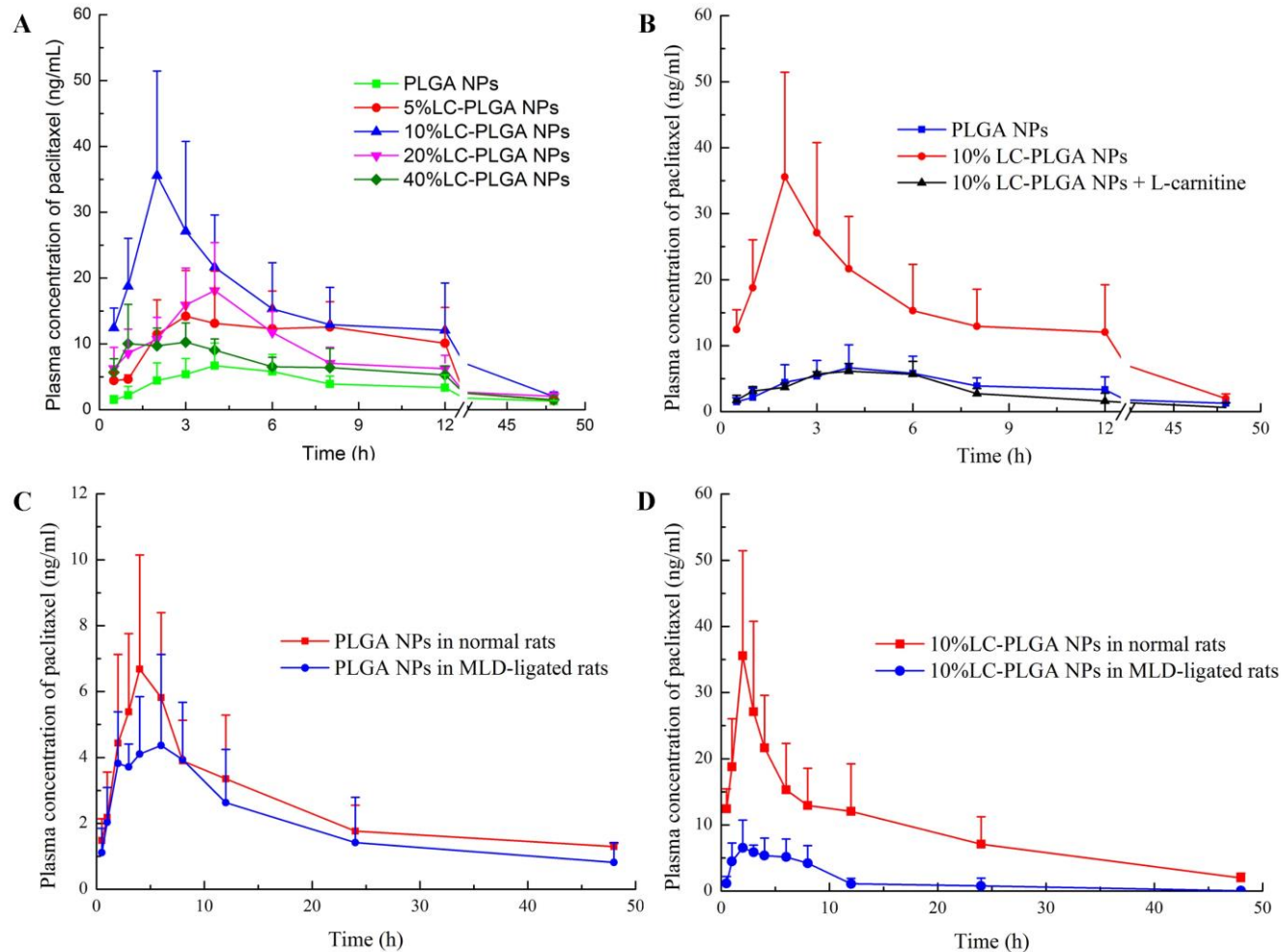
Pharmacokinetic profiles of paclitaxel in rats after oral administration. (A)Plasma levels of paclitaxel following oral administration of LC-PLGA NPs; (B)Plasma levels of paclitaxel following oral administration of 10% LC-PLGA NPs with free L-carnitine; plasma concentration-time curves for paclitaxel in normal and MLD-ligated rats after oral administration of PLGA NPs (C) and 10% LC-PLGA NPs (D).

L-Carnitine-conjugated NPs: Conclusions

L-Carnitine-conjugated NPs for interaction with OCTN2 and ATB$^{0,+}$

Table 1. The difference of OCTN2 and ATB$^{0,+}$ in the transport of L-carnitine.

Name	Gene	Tissue expression	Ion-dependence	K_m(L-carnitine)
OCTN2(human)	SLC22A5	Intestine, rain, heart, kidney, liver, pancreas, lung, thyroid, trachea, etc.	Na$^+$-dependent	4.3μM
octn2(mouse)	slc22a5			22.1 μM
ATB$^{0,+}$(human)	SLC6A14	Lung, hippocampus, stomach, prostate, pituitary, uterus, heart, colon, caecum	Na$^+$ and Cl$^-$ -dependent	
atb$^{0,+}$(mouse)	slc6a14			830 μM

LC-PLGA NPs

OCTN2   ATB$^{0,+}$
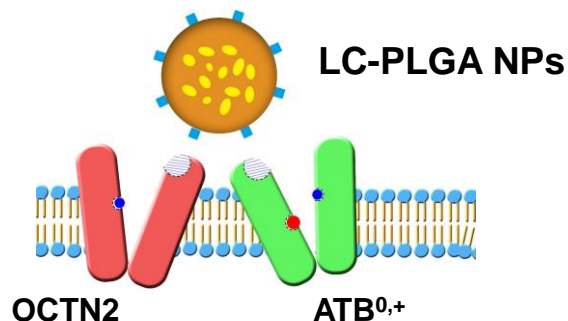
Amino acid nutrition in cancer

Essential amino acids

- Protein synthesis to promote cell proliferation

Leucine

- A potent activator of mTORC1; Signaling of sufficient nutrition
- Promotion of protein synthesis and hence cell proliferation
- mTOR inhibitors in clinical use for cancer treatment

Glutamine

- A critical amino acid for purine and pyrimidine synthesis
- The starting substrate for "glutaminolysis" unique to tumor cells
- Also an activator of mTORC1, though less potent than leucine
- Blockade of glutaminase inhibits tumor growth

Serine, Glycine, Proline, and Asparagine

- Promotion of tumor growth

Amino acid transporters that are upregulated in cancer

- **SLC1A5 (ASCT2)**

Alanine-Serine-Cysteine Transporter 2

- **SLC7A5 (LAT1)**

System L Amino acid Transporter 1

- **SLC7A11 (xCT)**
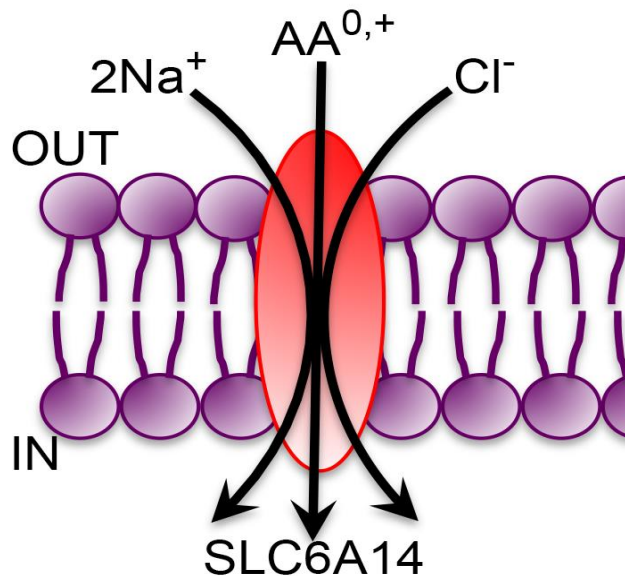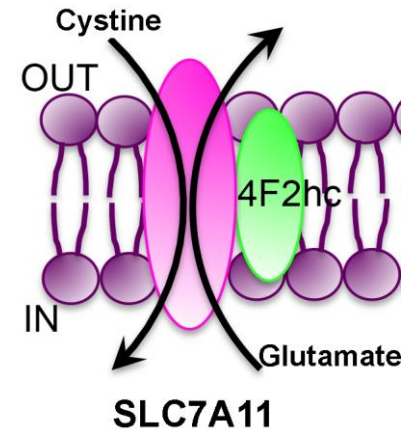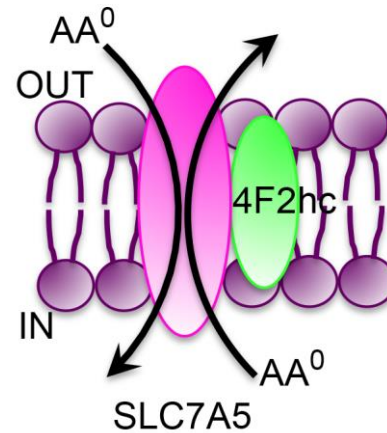
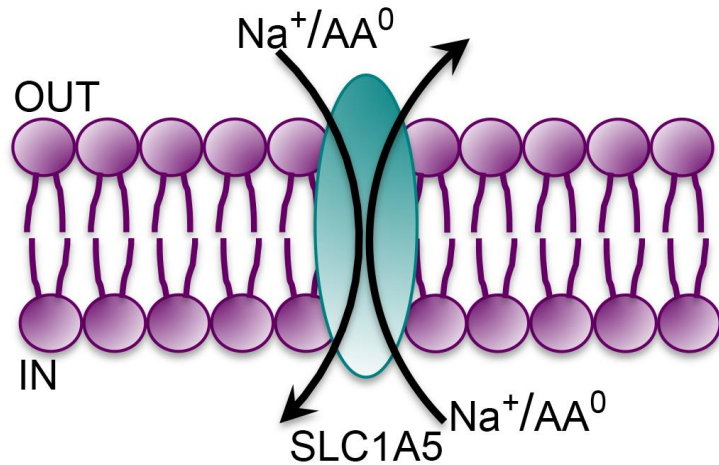**Cystine-glutamate exchanger; x_c Transporter**

- **SLC6A14 (ATB$^{0,+}$)**

Amino acid Transporter B$^{0,+}$

- **SLC38A5 (SN2)**

System N transporter 2

Amino acid transporters relevant to cancer: Functional features
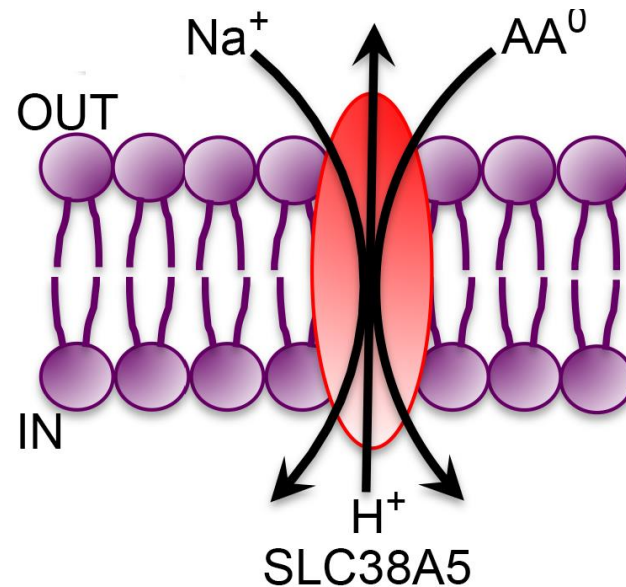
ATB$^{0,+}$ (SLC6A14)

Pros

ATB$^{0,+}$ is upregulated in several cancers

ATB$^{0,+}$ transports glutamine as well as all essential amino
acids, including lysine, in a Na$^+$/Cl$^-$ -coupled manner

Blockade of ATB$^{0,+}$ causes amino acid starvation and
suppresses mTORC1 signaling

Blockade of ATB$^{0,+}$ should interfere with tumor growth

Deletion of Slc6a14 in mice has no overt phenotype

Supporting data with cancer cell lines as well as with
spontaneous tumors

Cons

ATB$^{0,+}$ is upregulated only in selective types of cancers

Amino acid transporters in pancreatic cancer

Table 1. Changes in expression of SLC6A14, SLC7A5, SLC7A11 and SLC1A5 in pancreatic cancer

Data set	Glutamine transporter	Fold change	p value
GSE 19650	SLC6A14	95.03	0.0001
	SLC7A5	1.09	0.1699
	SLC7A11	3.97	0.0025
	SLC1A5	1.46	0.199
GSE 15471	SLC6A14	14.61	$1.5 \times e^{-10}$
	SLC7A5	1.55	0.0001
	SLC7A11	0.85	0.026
	SLC1A5	1.05	0.1232
GSE 16515	SLC6A14	39.51	$1.95 \times e^{-14}$
	SLC7A5	2.02	0.005
	SLC7A11	1.97	0.0002
	SLC1A5	1.28	0.0013
GSE 28735	SLC6A14	13.37	$1.88 \times e^{-14}$
	SLC7A5	1.44	0.0089
	SLC7A11	1.81	0.0001
	SLC1A5	1.2	0.0025
GSE 32676	SLC6A14	163.31	0.0001
	SLC7A5	0.34	0.0315
	SLC7A11	3.1	0.0009
	SLC1A5	1.26	0.3324
GSE 19279	SLC6A14	1.33	0.0551
	SLC7A5	1.75	0.0038
	SLC7A11	0.72	0.0052
	SLC1A5	0.99	0.2869
GSE 39751	SLC6A14	1.23	0.0496
	SLC7A5	1.3	0.258
	SLC7A11	0.93	0.196
	SLC1A5	1	0.3702
GSE 43288-GPL96	SLC6A14	1.29	0.0507
	SLC7A5	1.71	0.0107
	SLC7A11		
	SLC1A5	0.96	0.3909

Amino-acid-conjugated liposomes to deliver chemotherapy agents into SLC6A14-positive tumors
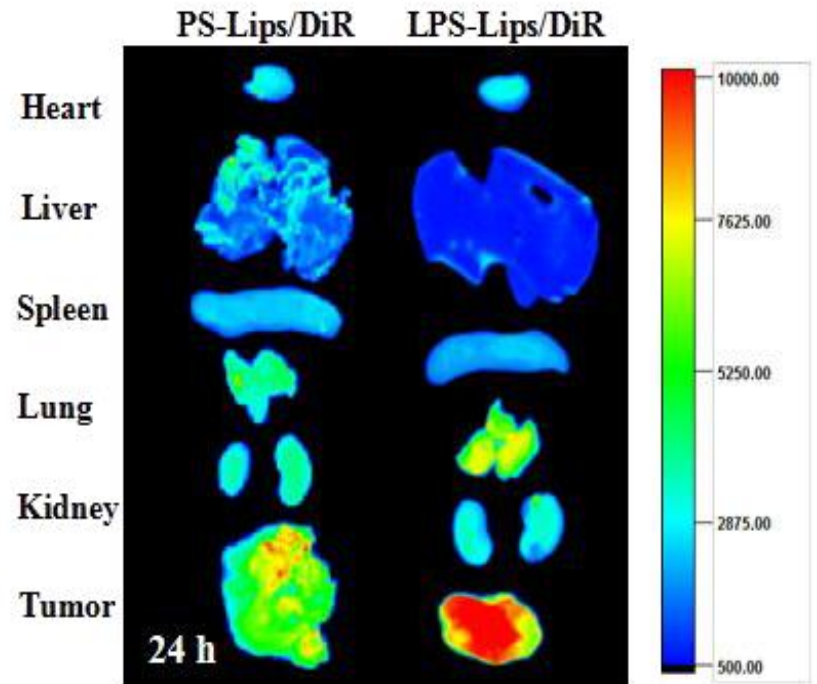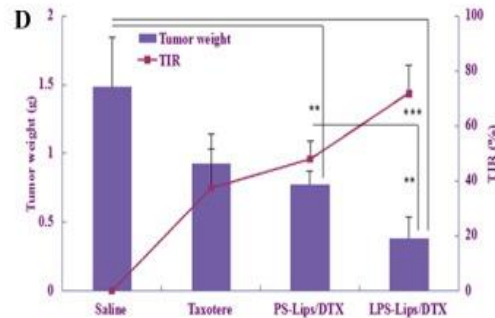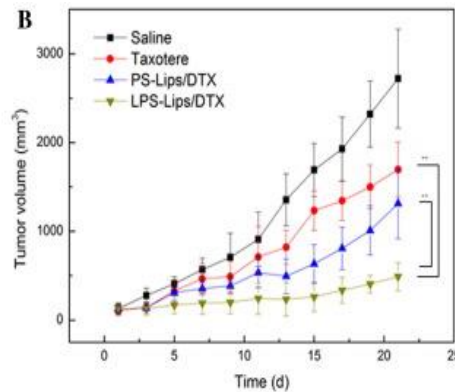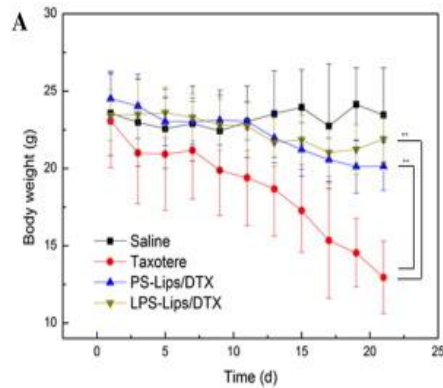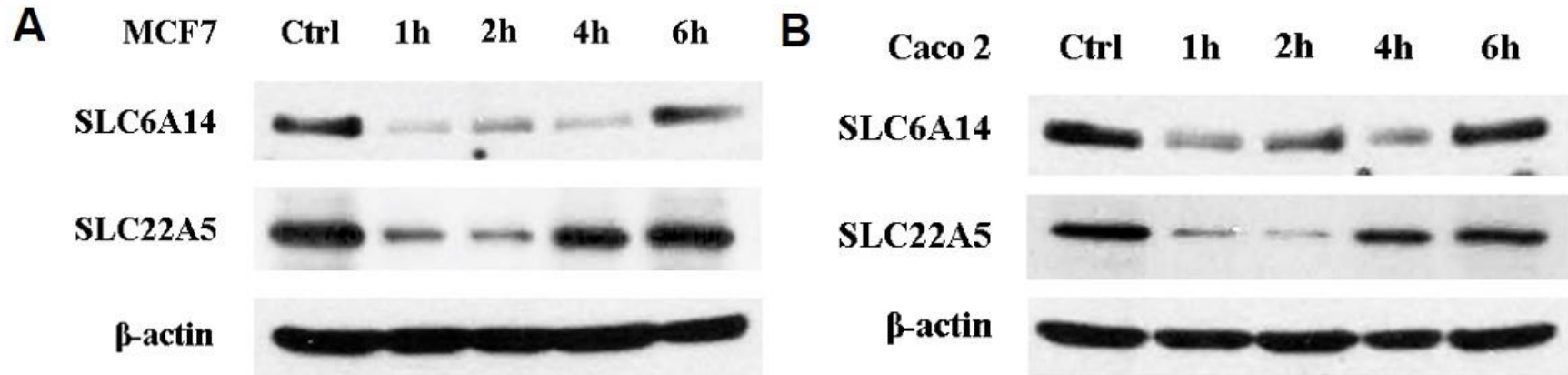
L-Carnitine-conjugated NPs: Evidence for interaction with OCTN2 and ATB$^{0,+}$
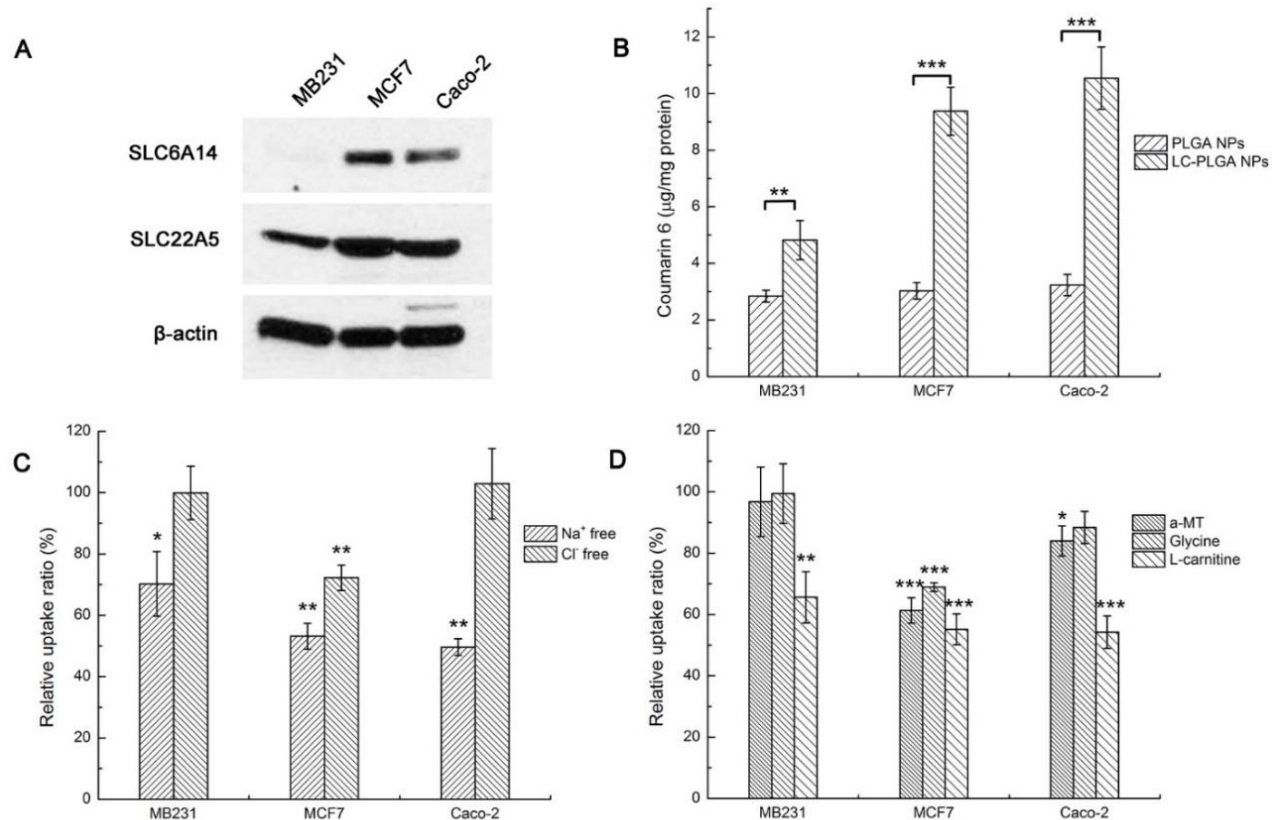
A, Expression of OCTN2 (SLC22A5) and ATB$^{0,+}$ (SLC6A14) proteins in MB231, MCF7 and Caco-2 cells, with β-actin as an internal control; B, Uptake of coumarin 6 from bare nanoparticles (PLGA NPs) and L-carnitine conjugated nanoparticles (LC-PLGA NPs) in these three cell lines; C, Effect of Na$^+$ and Cl$^-$ on the uptake of coumarin 6 from LC-PLGA NPs; D, Effect of specific inhibitors (α-MT and glycine for ATB$^{0,+}$, L-carnitine for OCTN2) on the uptake of coumarin 6 from LC-PLGA NPs.
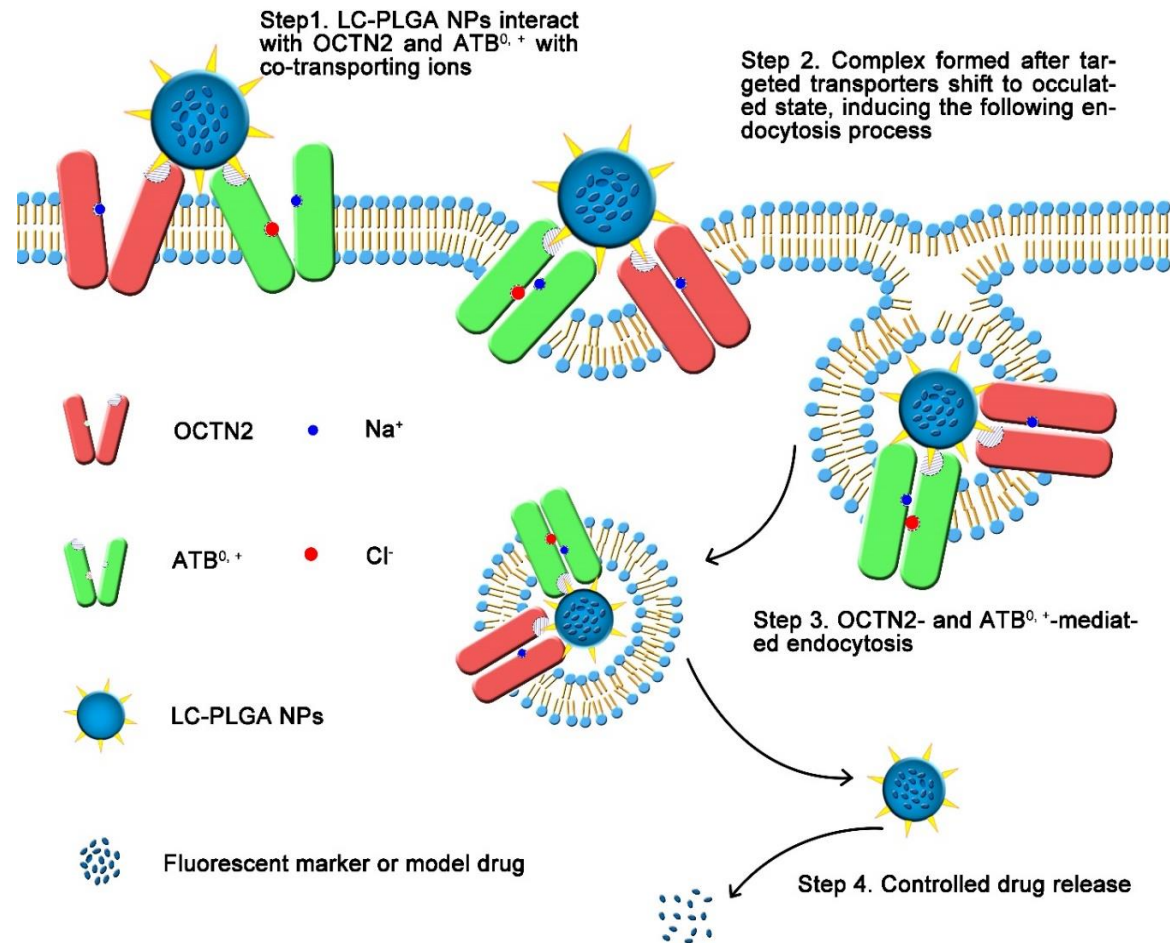
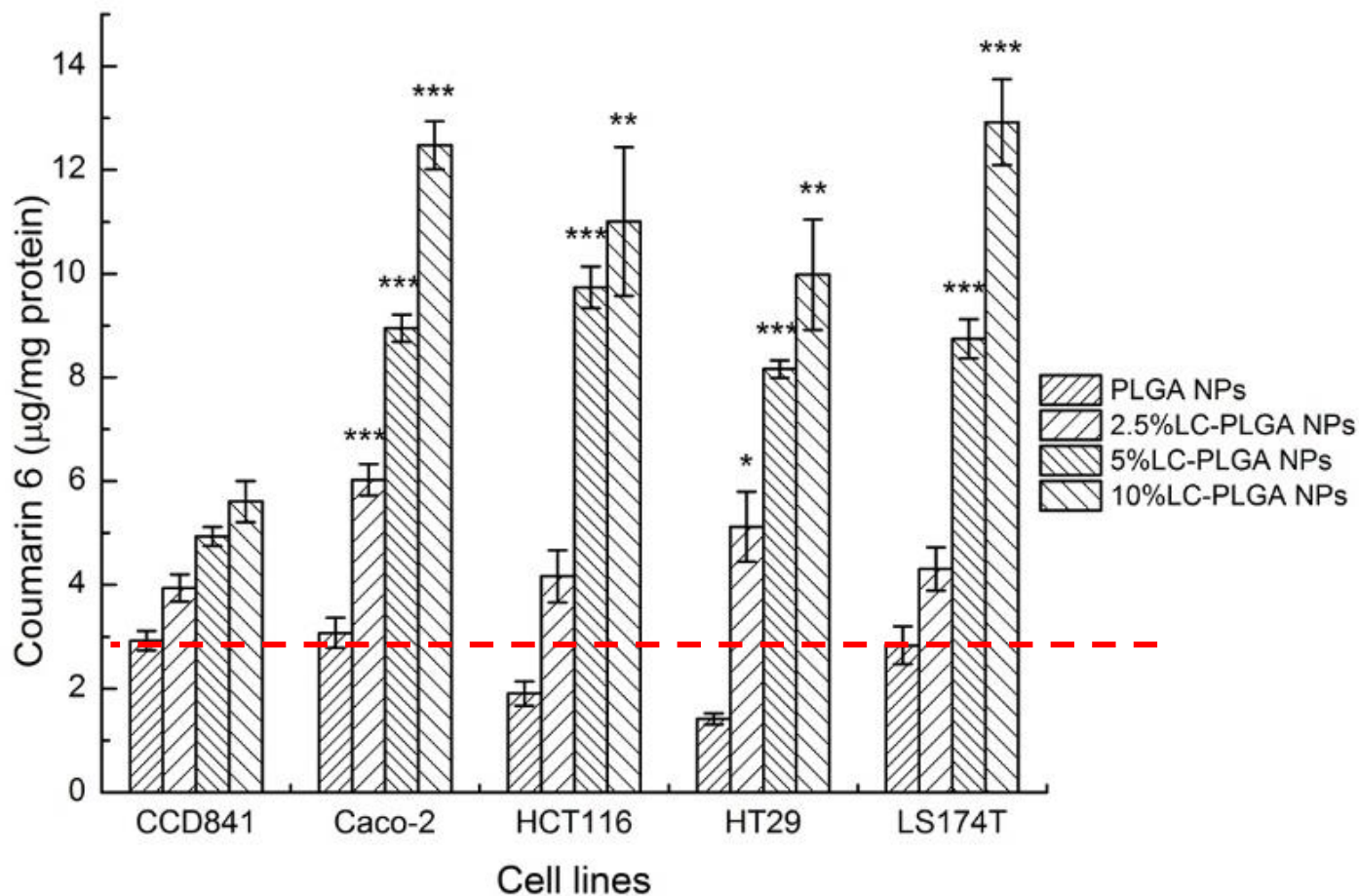# L-Carnitine-conjugated NPs: Interaction with OCTN2 and ATB$^{0,+}$

The protein levels of OCTN2 and ATB$^{0,+}$ in A) MCF7 cells and B) Caco-2 cells after treatment with LC-PLGA NPs for different time periods.

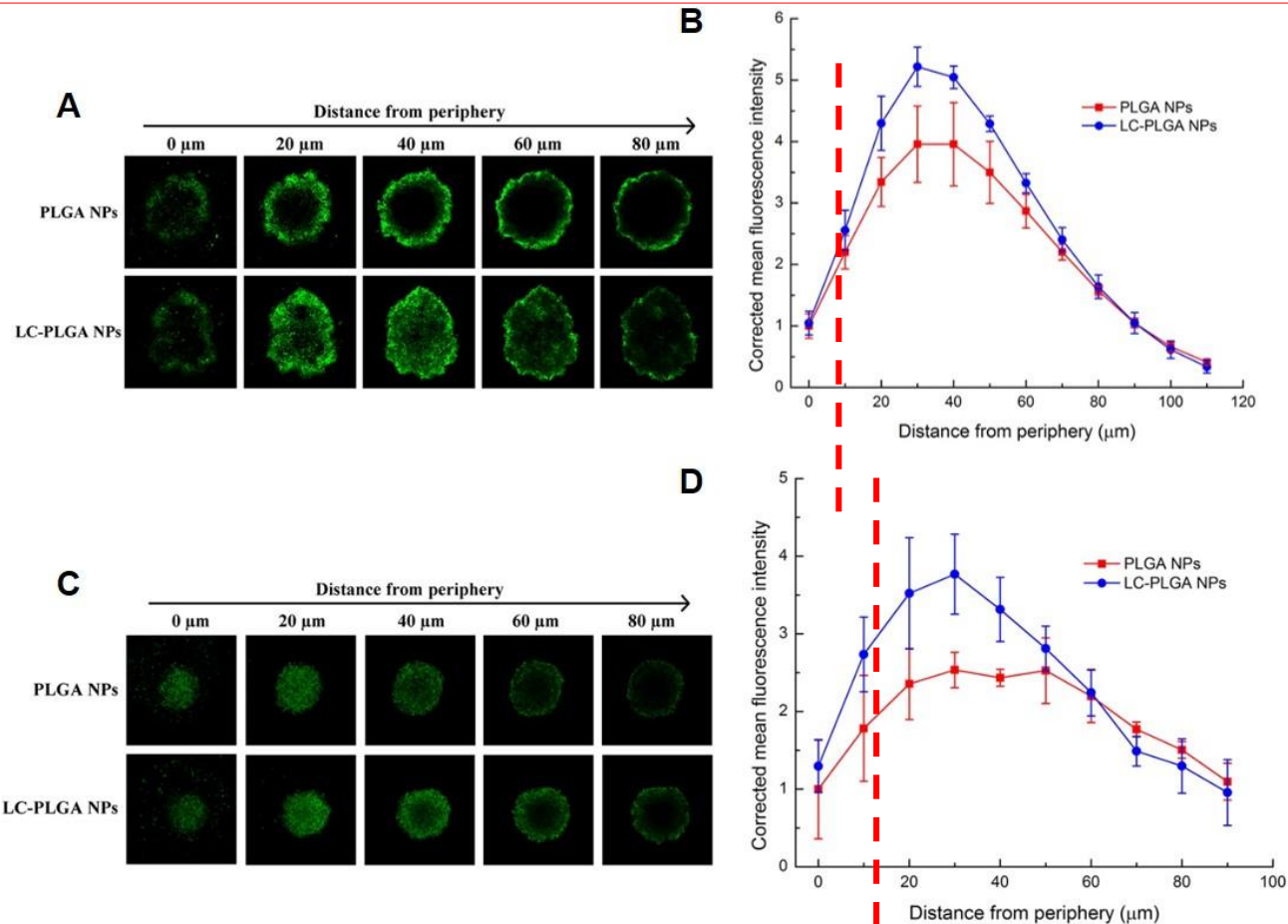**Potential mechanism for LC-PLGA NPs targeting to OCTN2 and ATB$^{0,+}$**

Uptake of coumarin 6 from LC-PLGA NPs with different ligand density (0 to 10%) in colon cells. Data are shown as mean $\pm$ SD, n = 3. *, P < 0.05, **, P < 0.01, ***, P < 0.001, compared to uptake in normal colon cells (CCD841).

Coumarin-6-loaded L-Carnitine-conjugated NPs: Penetration in cancer cell 3D spheroids

Nanoparticle penetration of spheroids. Z-stack images taken by confocal microscopy showing penetration of coumarin 6-labeled PLGA NPs and LC-PLGA NPs in A) HCT116 spheroids and C) HT29 spheroids. Green color indicates coumarin 6-labeled nanoparticles; Corrected coumarin 6 flourescence intensity represents the nanoparticles in B) HCT116 spheroids and D) HT29 spheroids from periphery to the inner layer. Data are shown as mean $\pm$ SD, (n = 3).

5'-FU-loaded L-carnitine-conjugated NPs: antitumor efficacy in 3D spheroids

Anti-tumor efficiency in 3D spheroids
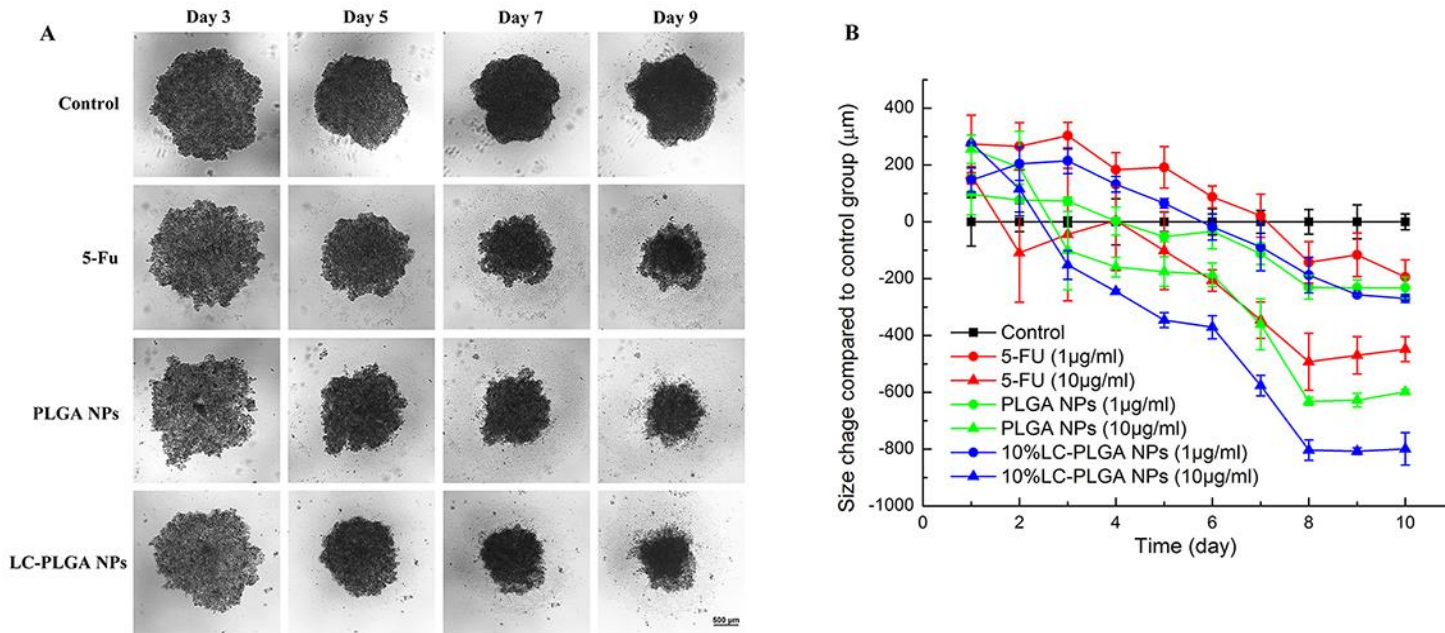
Spheroids treatment with free 5-FU, 5-FU-loaded PLGA NPs and 5-FU-loaded 10%LC-PLGA NPs. A, Morphological change in HCT116 spheroids during 10-day treatment with 10 µg/mL of free 5-FU, 5-FU-loaded PLGA NPs and 5-FU-loaded LC-PLGA NPs; B, Compared to control group, the size change of HCT116 spheroids treatment with 1 µg/mL and 10 µg/mL of free 5-FU, 5-FU-loaded PLGA NPs and 5-FU-loaded LC-PLGA NPs (n = 3).

A caution about the type of synthetic polymer used for NPs?

PLGA is used widely for generation of NPs
It is biodegradable and biocompatible
It produces lactic acid during biodegradation

Lactate is a tumor promoter by serving as the endogenous agonist for the cell-surface GPCR GPR81

Is this good for tumor-targeted delivery of anticancer drugs?

Alternative???

Poly(beta-hydroxybutyric acid)
It is also biodegradable and biocompatible
It produces beta-hydroxybutyrate during biodegradation

Beta-hydroxybutyrate is the endogenous agonist for the cell-surface GPCR GPR109A, a tumor suppressor